Natural Resources Canada | Ressources naturelles Canada

GEOLOGICAL SURVEY OF CANADA
OPEN FILE 8754

# Datasets in support of prospectivity modelling for magmatic Ni (± Cu ± Co ± PGE) mineral systems

C.J.M. Lawley, V. Tschirhart, J. Smith, E.M. Schetselaar,
A.J. Schaeffer, and B.M. Eglington

2021

Canada

GEOLOGICAL SURVEY OF CANADA
OPEN FILE 8754

# Datasets in support of prospectivity modelling for magmatic Ni (± Cu ± Co ± PGE) mineral systems

**C.J.M. Lawley[1], V. Tschirhart[1], J. Smith[1], E.M. Schetselaar[1], A.J. Schaeffer[2], and B.M. Eglington[3]**

[1]Geological Survey of Canada, 601 Booth Street, Ottawa, Ontario
[2]Geological Survey of Canada, 9860 West Saanich Road, Sidney, British Columbia
[3]Department of Geological Sciences, University of Saskatchewan, 114 Science Place, Saskatoon, Saskatchewan

## 2021



Permanent link: https://doi.org/10.4095/327573

This publication is available for free download through GEOSCAN (https://geoscan.nrcan.gc.ca/).

**Recommended citation**
Lawley, C.J.M., Tschirhart, V., Smith, J., Schetselaar, E.M., Schaeffer, A.J., and Eglington, B.M., 2021. Datasets in support of prospectivity modelling for magmatic Ni (± Cu ± Co ± PGE) mineral systems; Geological Survey of Canada, Open File 8754, 1 .zip file. https://doi.org/10.4095/327573

Publications in this series have not been edited; they are released as submitted by the author.

## Introduction

The Geological Survey of Canada (GSC) has provided geoscience data in support of the Canadian mineral exploration industry since its founding in 1842 (Lebel, 2019). The vast majority of GSC research results have been made publically available, either through scientific publications in peer-reviewed journals, digital datasets that are available for download on the GEOSCAN publication database, or, more recently, as online digital data repositories (Teskey and Hood, 1991; Teskey, 1993; Boisvert and Brodaric, 2012; Adcock et al., 2013; Courtney, 2013). Online repositories typically represent data collected over many decades from multiple sources of government, academic, and/or industry research. Examples of GSC-maintained online digital data repositories include the Canadian Database of Geochemical Surveys (https://geochem.nrcan.gc.ca), the Geoscience Data Repository for Geophysical Data (http://gdr.agg.nrcan.gc.ca), the Canadian Geochronology Knowledgebase (CGKB; https://www.nrcan.gc.ca/maps-tools-publications/tools/geodetic-reference-systems/canadian-geochronology-knowledgebase/18211), and the Groundwater Information Network (https://gin.gw-info.net/service/api_ngwds:gin2/en/gin.html). Each of these databases provide users with a single repository for accessing modern and legacy surveys. Some of these databases also make curated survey compilations available for download and, in the case of gravity and magnetic datasets, provide near complete coverage of the Canadian landmass (Fig. 1).

Historically, individual research groups developed and maintained their own separate databases, which, over time, has led to major differences in the structure, format, and content of the online repositories. These differences, coupled with data quality issues and changes in survey design and analytical methods over time, present significant challenges for integrating data from multiple sources. Herein we address some of the challenges that are specific to data integration and present a compilation of public geological, geophysical, geochemical, and geochronological datasets from across Canada. Each of these datasets were downloaded in their original format from multiple sources (e.g., GSC and other government and academic sources), processed (e.g., derivative products, statistical transformations, missing value replacement), and re-sampled (i.e., zonal statistics) into a common 5 x 5 km grid (Table 1). The final geospatial grid represents a map of Canada with each row representing a single map pixel (n = 395,088 pixels) and each column representing a separate dataset (Table 2). Larger and more complex examples of this multidimensional and/or spatiotemporal data structure are known as a "data cube" and represent an important product for conveying geological survey data in a simplified digital format (Lewis et al., 2017). Re-sampling individual datasets to a common grid also provides a mechanism for integrating each of the main geological, geophysical, and geochemical GSC-hosted data repositories into a single digital table (i.e., comma separated value, csv; Table 2).

The combined dataset reported in Table 2, coupled with advanced machine learning tools, can be applied to address multiple geoscience research areas (e.g., land-use planning, remote predictive mapping, and cumulative effects). For example, Lawley et al. (in press) used the re-gridded data in Table 2 and the $H_2O$ Artificial Intelligence platform (Aiello et al., 2016) to generate Canada's first mineral potential model for magmatic Ni (± Cu ± Co ± PGE) mineral systems. The relatively coarse resolution of the grid (5 x 5 km) means that data reported in Table 2 are best suited for reconnaissance and/or continent-scale applications.

## Datasets

A guide to the datasets included as part of the current study is reported in Table 1. All of the re-gridded datasets are reported in Table 2. Data are presented using the Canada Atlas Lambert coordinate system (EPSG:3978). Most of these re-processed datasets in Table 2 were compiled from GSC databases. Other datasets were collected from provincial and territorial databases (i.e., mineral occurrences) and academic sources (i.e., geological terranes; Eglington et al., 2009; Eglington et al., 2013). New datasets and derivative products are also reported here for the first time (e.g., potential field compilation maps, multi-scale edge detection, age map, and proximity surfaces). Some datasets that were originally downloaded in a vector file format were rasterized for the purposes of prospectivity modelling (discussed further below).

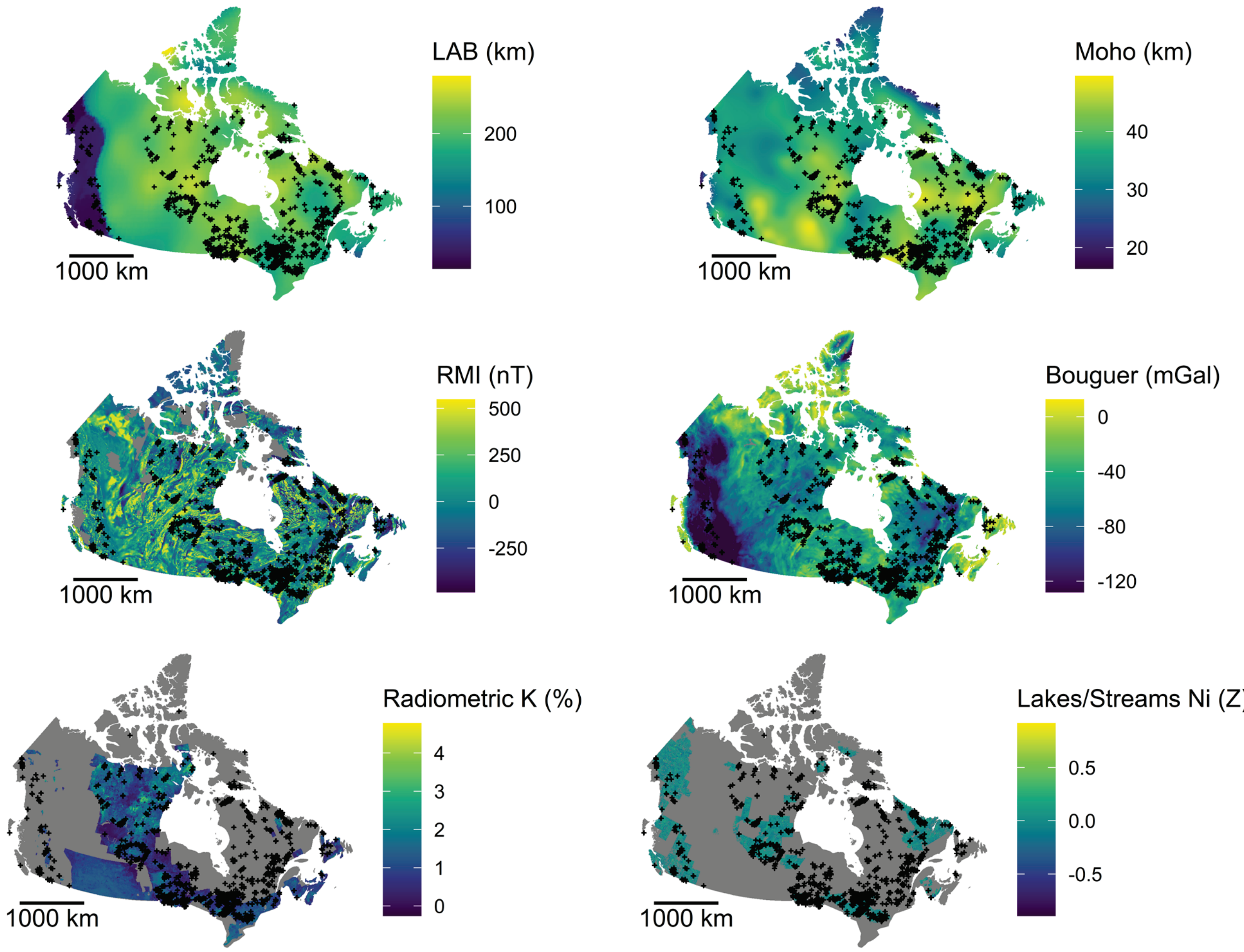


*Figure 1: Maps showing the distribution of seismic (e.g., depth to the lithosphere-asthenosphere boundary, LAB; depth to the Mohorovičić discontinuity, Moho), magnetic (e.g., residual magnetic intensity, RMI), gravity (e.g., Bouguer), radiometric (e.g., K) and geochemistry (e.g., lake and stream sediment geochemistry concentrations transformed to Z scores). Missing values are shown in grey. The combined Ni mineral occurrence database is shown for reference (crosses).*

**Ni mineral occurrences**

Known Ni deposits, prospects, and showings were compiled from provincial, territorial, and previously published national mineral occurrence databases (Good et al., 2015) and are hereafter referred to as "Ni mineral occurrences". Individual mineral occurrence databases were filtered to include Ni as the primary or secondary commodity. The commodity filtered dataset was manually edited to remove entries with spurious element associations (e.g., Ni + U, Ni + Pb + Zn, and Ni + Co + Bi) that are unlikely to reflect the magmatic Ni (± Cu ± Co ± PGE) mineral system. This process typically removed Ni mineral occurrences that have genetic affinities with volcanogenic massive sulphide (VMS), unconformity U, and polymetallic vein-type mineral systems. The commodity filtered dataset was also plotted and edited manually to remove Ni mineral occurrences within the Sudbury Basin. Despite this effort, the filtered dataset is still expected to contain an unknown proportion of Ni mineral occurrences that are unrelated to the mineral system of interest. Hydrothermal and polymetallic vein-type mineral systems proved very difficult to identify with confidence on the basis of their primary and secondary commodities and other limited metadata. The final compiled dataset also represents a mix of mafic to ultramafic rock-associated mineral system subtypes (e.g., Alaska-type; Komatiite-associated; rift-related; hydrothermal awaruite-hosted; Naldrett, 1999; Naldrett, 2004; Eckstrand and Hulbert, 2007) that show considerable variation in terms of their economic significance (e.g., pentlandite-bearing outcrop, significant drill intersections, and giant Ni deposits such as Raglan). The final compiled database (n = 1,939) is assumed to represent locales of known potential for mafic to ultramafic rock-associated mineral systems and were used as training data for the national prospectivity model (Table 2).

**Geological datasets**

Geological provinces, geological ages, rock types, and faults were taken from the digital compilation of Wheeler et al. (1996), which provides complete coverage of the Canadian landmass and some offshore areas. Rock types are based on the "SUBRXTP" field and are sub-divided into 49 separate categories. These rock types were re-grouped into a smaller subset of categories (n = 10) based on their rock association and relative Ni prospectivity (i.e., ultramafic mix high, mafic mix high, volcanic-sedimentary mix high, volcanic-sedimentary mix moderate, volcanic-sedimentary mix low, granite mix moderate, granite mix low, gneiss mix, sedimentary mix low, and mix low). The prospectivity of each rock type for magmatic Ni sulphide deposits is discussed in Lawley et al. (in press). Fault data (Wheeler et al., 1996) and surficial traces of geological terranes (Eglington et al., 2009; Eglington et al., 2013; Pehrsson et al., 2013) were converted to a continuous proximity surface (m) for the purpose of prospectivity modelling (Table 2).

**Geophysical datasets**

The GSC (including the former Earth Physics Branch) has been continuously acquiring gravity data since 1944. Ground stations correspond to an average spacing of 10–15 km. Data are freely available for download from the Geoscience Data Repository for Geophysical Data. Canadian gravity data are tied to the International Gravity Standardization Network 1971 (IGSN71) and are corrected for latitude, instrument drift, elevation, and Earth's tides followed by application of the Free Air and Bouguer corrections as described in Jobin et al. (2017). Data are reported in mGal (milligal) and were reduced to a Bouguer slab density of 2.67 g/cm3 and gridded to 2 km using minimum curvature. Missing Bouguer values from areas that were not covered were stitched to the Canada Bouguer grid from data compiled as part of the World Gravity Map (Bonvalot et al., 2012) as part of the current study (Table 2).

Aeromagnetic data has been acquired since 1947 as part of Canada's National Aeromagnetic Surveying program. Initial surveys were flown along 805 m-spaced lines at 300 m elevation and covered large areas of the Canadian landmass. More recent surveys were collected at closer line spacing (400–200 m-spaced lines) and followed modern acquisition parameters as described in Miles and Oneschuk (2016). Modern and legacy magnetic datasets are reported in nT (nanoteslas). New surveys are continuously levelled and merged as they become available and gridded to 200 m using minimum curvature. The updated data is available through the Geoscience Data Repository for Geophysical Data. Missing values from areas that were not covered by systematic surveying were stitched using data from the World Digital Magnetic Anomaly Map project (Dyment et al., 2015) as part of the current study (Table 2).

Derivatives and their products (e.g., tilt, 1st vertical derivative, 1VD; horizontal gradient magnitude, HGM) were calculated on the stitched magnetic (RMI; Residual Magnetic Intensity) and Bouguer gravity grids to enhance textures, the locations of structures and contacts, and shorter wavelength anomalies. These techniques maximize some function over the edge or centre of a source body, provided there is sufficient contrast between the magnetic susceptibilities or densities (i.e., magnetic and gravity data, respectively) of laterally adjacent source bodies. The 1VD removes the long wavelength regional component of the potential field thereby enhancing short wavelength features and is useful for delineating the edges of source bodies and near surface structures (Dentith and Mudge, 2014). The HGM is the sum of the full horizontal gradient and can effectively delineate the edges of contacts or structures (Cordell and Grauch, 1985; Fairhead, 2016) and tilt is a normalizing technique that is positive over the magnetic source, zero at the edges, and negative outside the source (Miller and Singh, 1994). Normalizing techniques have the advantage of equally enhancing sources located at depth and at surface.

Additional processing included multi-scale edge analysis or 'worming'. Multi-scale edges were constructed from the maxima of the pseudo-gravity horizontal gradient grid (for the Canadian magnetic data) and HGM (for the Canadian gravity data) for a series of upward continuation levels (Holden et al., 2000). The location of the maxima at each upward continuation level represents anomalies located at greater than half the upward continuation distance (i.e., maxima at a 5000 m upward continuation level reflects features 2500 m or deeper). Multi-scale edges migrate outward in the down-dip direction at increasing upward continuation levels, providing information on the dip direction and subsurface geometry. Proximity surfaces for each continuation level were generated for the purposes of prospectivity modelling.

Airborne gamma-ray spectrometry data have been acquired since 1970 with flight lines ranging from 200–25000 m. Data were processed to generate the natural air absorbed dose rate, concentrations at ground level of K (%), Th (ppm), and U (ppm), as well as ratios of these elements to one another, and gridded to 250 m using minimum curvature. Details on the compilation and processing of datasets used in this study are found in Buckle et al. (2014a; 2014c; 2014d; 2014b). Missing values were imputed with a zero value after converting all radiometric data to Z-scores (i.e., mean-centered and normalized by standard deviation). Future research will investigate whether alternative data normalizing techniques, which are better suited for non-normal datasets, have the potential to improve prospectivity modelling results (Lawley et al., in press).

Seismic data was used to interpret the approximate the location of deeper geological boundaries, including the base of the continental crust (i.e., the Mohorovičić discontinuity or Moho) and the lithosphere-asthenosphere boundary (LAB). The data and methods used to estimate crustal and lithospheric thickness (km) have been previous reported in Schetselaar and Snyder (2017) and Schaeffer and Lebedev (2014), respectively (Table 2). Uncertainties and the resolution of the Canadian Moho are discussed in Snyder et al. (2018). Upper mantle seismic velocities at 50 km intervals (50–300 km) were also used to infer other upper mantle features (e.g., discontinuities, thermal erosion, metasomatism; Table 2; Yuan et al., 2014).

**Geochemical datasets**

Lake and stream sediment data were downloaded and compiled from the Canadian Database of Geochemical Surveys (Adcock et al., 2013). Individual surveys included within this database were collected from the 1950s and continued as part of the former National Geochemical Reconnaissance Project (Friske and Hornbrook, 1991; Painter et al., 1994; Adcock et al., 2013). Scripts were written as part of the current study to compile several of the most common elements (e.g., Mg, Fe, Mn, Ni, Cu, Co) included within this large database (i.e., selected elements represent 2,197,184 data points). Because element concentrations vary systematically with sample media (e.g., grain size, sediment type), digestion methods (e.g., aqua-regia, four-acid, fusion), and analytical methods (e.g., instrumental neutron activation analysis, inductively coupled plasma emission spectroscopy, inductively coupled plasma mass spectrometry), multiple processing steps were required to integrate the data. First, data for each element were subdivided into partial ("partial aqua-regia" and "partial fusion") and complete ("total" and "none") digestion methods. Raw concentration data were then transformed to Z-scores for each combination of survey and analytical method using the "Survey" and "Bundle" codes, respectively. This data transformation step attempts to address some of the systematic variation in analytical methods over time, but has adverse effects for surveys that are dominated by a single rock type. More advanced data levelling techniques would require the same reference materials to be analyzed for each survey over time (Grunsky, 2010), which is currently not possible for all areas of Canada. Calculated Z-scores for partial digestion data were then interpolated using an inverse weighted distance (IWD) method and clipped to the approximate spatial extent of each survey group. All remaining missing values for areas that are not surveyed were imputed with a zero value.

**Geological ages**

Geochronology data were taken from the Canadian Geochronology Knowledgebase at the GSC. Ages included within this database were collected from government publications and academic research. Data were filtered to include crystallization and other interpreted protolith ages and comprise multiple analytical methods, radiogenic systems, and geochronometers (n = 8,569). Geochronology results were then spatially joined to the geology map in order to compare the calculated mean age for each rock polygon to the age estimates provided by Wheeler et al. (1996). Geochronology ages that were greater or less than the maximum and minimum age estimates for each rock polygon provided by Wheeler et al. (1996) were excluded. Comparing age estimates based on cross cutting relationships with geochronology results was used to exclude analyses that are unrelated to the local geology (e.g., dyke ages that are significantly younger than the host rocks). The final estimated age for each rock polygon thus represents an update of the Wheeler et al. (1996) dataset that are based on the best available constraints from the available geochronology results.

**<u>Data integration</u>**

All spatial operations and other data processing and plotting methods were completed in the free and open source R software environment (R Development Core Team, 2019). Data wrangling relied heavily on packages that are included within the tidyverse (Wickham et al., 2019) and are based on the principals of tidy data (Wickham, 2014). Spatial operations were mostly completed with the simple features (sf), velox, and raster packages. Raster data were re-gridded using the arithmetic "mean" function within velox; whereas geological polygon data were spatial joined to the 5 x 5 km grid using the sf package. Each grid cell contains a unique grid identification ("grid_id"), column identification ("col_id"), and row identification ("row_is") numbers. The coordinates of each cell center are reported in the Canada Atlas Lambert coordinate system (EPSG:3978). Column headers in Table 2 are named using the following scheme wherever possible: Method_Dataset_Unit. Missing values are reported as "NA". Imputed datasets are highlighted as column header names with the suffix "imp". The full legend for linking column headers to the re-gridded datasets is reported in Table 1.

Each row in the combined dataset (Table 2) represents the cumulative knowledge of that particular 5 x 5 km area of Canada and, coupled with machine learning tools, can be used to build predictive models for a large number of applications. Machine learning tools are particularly effective at finding hidden patterns between variables within the combined datasets. These patterns would have been impossible to identify had each of the input geological, geochemical, and geophysical datasets been interpreted separately. The integrated data developed as part of the current study can effectively reduce the search space for magmatic Ni mineral systems (i.e., the preferred prospectivity model suggest that 8% of map pixels contains more than 80% of known Ni mineralization; Lawley et al., in press). Future research will focus on further developing the process and technology for integrating GSC datasets with other data sources to improve prospectivity model results.

**Acknowledgments**

Many of the datasets reported herein were acquired over many decades. Thank you to all of the GSC scientists, staff, and students that have made this work possible. The vast majority of GSC research also requires close collaboration with other government (e.g., provincial and territorial governments), academic, and industry partnerships. Thank you to all of the collaborators that have contributed to the data presented herein. Christopher Stevens, Azadeh Ashoori Pareshkoohi, and Aeron Vaillancourt are thanked for their assistance with data compilation and processing. Funding was provided by the Targeted Geoscience Initiative (TGI) program. The manuscript befitted from an internal review by Michael Gadd.

**References**

Adcock, S. W., Spirito, W. A., and Garrett, R. G., 2013, Geochemical data management – issues and solutions: Geochemistry: Exploration, Environment, Analysis, v. 13, p. 337–348.

Aiello, S., Eckstrand, E., Fu, A., Landry, M., and Aboyoun, P., 2016, Machine Learning with R and H2O (J. Lanford, Ed.): Mountain View, CA, H2O.ai, 45 p.

Boisvert, E., and Brodaric, B., 2012, GroundWater Markup Language (GWML) - Enabling groundwater data interoperability in spatial data infrastructures: Journal of Hydroinformatics, v.

14, p. 93–107.

Bonvalot, S., Balmino, G., Briais, A., Kuhn, M., Peyrefitte, A., Vales, N., Biancale, R., Gabalda, G., Reinquin, F., Sarrailh, M., and Reinquin, G., 2012, World Gravity Map: Commission for the Geological Map of the World.

Buckle, J., Carson, J., Ford, K., Fortin, R., and Miles, W., 2014a, Radioactivity map of Canada, natural air absorbed dose rate: Geological Survey of Canada, Open File 7396, 1 sheet, 1:5000000.

Buckle, J., Carson, J., Ford, K., Fortin, R., and Miles, W., 2014b, Radioactivity map of Canada, potassium: Geological Survey of Canada, Open File 7403, 1 sheet, scale 1:5000000.

Buckle, J., Carson, J., Ford, K., Fortin, R., and Miles, W., 2014c, Radioactivity map of Canada, thorium: Geological Survey of Canada, Open File 7401, 1 sheet, scale 1:5000000.

Buckle, J., Carson, J., Ford, K., Fortin, R., and Miles, W., 2014d, Radioactivity map of Canada, uranium: Radioactivity Map of Canada, Uranium; Geological Survey of Canada, Open File 7402, 1 sheet, scale 1:5000000.

Cordell, L., and Grauch, V., 1985, Mapping basement magnetization zones from aeromagnetic data in the San Juan basin, New Mexico, in Hinze, W. ed., The Utility of Regional Gravity and Magnetic Anomaly Maps: Society of Exploration Geophysicists, p. 181–197.

Courtney, R., 2013, Canada GEESE 2. Visualization of Integrated Marine Geoscience Data for Canadian and Proximal Waters: Geoscience Canada, v. 40, p. 141–148.

Dentith, M., and Mudge, S., 2014, Geophysics for the Mineral Exploration Geoscientist: Cambridge University Press, 438 p.

Dyment, J., Lesur, V., Hamoudi, M., Choi, Y., Thebault, E., and Catalan, M., 2015, The WDMAM Task Force*, the WDMAM Evaluators**, and the WDMAM Data Providers**: World Digital Magnetic Anomaly Map version 2.0.

Eckstrand, R., and Hulbert, L., 2007, Magmatic nickel-copper-platinum group element deposits, in Mineral Deposits of Canada: A Synthesis of Major Deposit-Types, District Metallogeny, the Evolution of Geological Provinces, and Exploration Methods: Geological Association of Canada, p. 205–222.

Eglington, B., Reddy, S., and Evans, D., 2009, The IGCP 509 database system: design and application of a tool to capture and illustrate litho- and chrono-stratigraphic information for Palaeoproterozoic tectonic domains, large igneous provinces and ore deposits; with examples from southern Africa, in Reddy, S., Mazumder, R., Evans, D., and Collins, A. eds., Palaeoproterozoic Supercontinents and Global Evolution: Geological Society Special Publication 323, p. 27–47.

Eglington, B. M., Pehrsson, S. J., Ansdell, K. M., Lescuyer, J. L., Quirt, D., Milesi, J. P., and Brown, P., 2013, A domain-based digital summary of the evolution of the Palaeoproterozoic of North America and Greenland and associated unconformity-related uranium mineralization: Precambrian Research, v. 232, p. 4–26.

Fairhead, D., 2016, Advances in Gravity and Magnetic Processing and Interpretation: EAGE, 352 p.

Friske, P., and Hornbrook, E., 1991, Canada's national geochemical reconnaissance programme: Transactions of the Institution of Mining and Metallurgy Section B: Applied Earth Sciences, v. 100, p. B47–B56.

Good, D., Eckstrand, O., Yakubchuk, A., and Gall, Q., 2015, World Ni-Cu-PGE-Cr deposit database: Geological Survey of Canada, Open File 7766, p. 8.

Grunsky, E. C., 2010, The interpretation of geochemical survey data: Geochemistry: Exploration, Environment, Analysis, v. 10, p. 27–74.

Holden, D., Archibald, N., Boschetti, F., and Jessell, M., 2000, Inferring geological structures using wavelet-based multiscale edge analysis and forward models: Exploration Geophysics, v. 31, p. 617–621.

Jobin, D., Veronneau, M., and Miles, V., 2017, Gravity anomaly map, Canada: Geological Survey of Canada, Open File 8081; scale 1:7500000.

Lawley, C.J.M., Tschihart, V., Smith, J., Pehrsson, S.J., Schetselaar, E.M., Houlé, M., Schaeffer, A.J., and Eglington, B.M., in press, Prospectivity modelling of Canadian magmatic Ni (± Cu ± Co ± PGE) mineral systems: Ore Geology Reviews.

Lebel, D., 2019, Geological Survey of Canada 8.0: mapping the journey towards predictive geoscience: Geological Society, London, Special Publications, p. SP499-2019–79.

Lewis, A., Oliver, S., Lymburner, L., Evans, B., Wyborn, L., Mueller, N., Raevksi, G., Hooke, J., Woodcock, R., Sixsmith, J., Wu, W., Tan, P., Li, F., Killough, B., et al., 2017, The Australian Geoscience Data Cube — Foundations and lessons learned: Remote Sensing of Environment, v. 202, p. 276–292.

Miles, W., and Oneschuk, D., 2016, Magnetic anomaly map, Canada: Geological Survey of Canada, Open File 7799, 1 sheet.

Miller, H., and Singh, V., 1994, Potential field tilt — a new concept for location of potential field sources: Journal of Applied Geophysics, v. 32, p. 213–217.

Naldrett, A., 1999, World-class Ni-Cu-PGE deposits: key factors in their genesis: Mineralium Deposita, v. 34, p. 227–240.

Naldrett, A., 2004, Magmatic Sulfide Deposits: Geology, Geochemistry and Exploration: Springer, 727 p.

Painter, S., Cameron, E. M., Allan, R., and Rouse, J., 1994, Reconnaissance geochemistry and its environmental relevance: Journal of Geochemical Exploration, v. 51, p. 213–246.

Pehrsson, S. J., Berman, R. G., Eglington, B., and Rainbird, R., 2013, Two Neoarchean supercontinents revisited: The case for a Rae family of cratons: Precambrian Research, v. 232, p. 27–43.

R Development Core Team, 2019, R: A language and environment for statistical computing: R Foundation for Statistical Computing, Vienna, Austria. URL https://www.R-project.org/.

Schaeffer, A. J., and Lebedev, S., 2014, Imaging the North American continent using waveform inversion of global and USArray data: Earth and Planetary Science Letters, v. 402, p. 26–41.

Schetselaar, E., and Snyder, D., 2017, National database of Moho depth estimates estimates from seismic refraction and teleseismic surveys: Geological Survey of Canada, Open File 8243, p. 14.

Snyder, D. B., Schetselaar, E., Pilkington, M., and Schaeffer, A. J., 2018, Resolution and uncertainty in lithospheric 3-D geological models: Mineralogy and Petrology, v. 112, p. S133–S147.

Teskey, D., and Hood, P., 1991, The canadian aeromagnetic database: Evolution and applications to the definition of major crustal boundaries: Tectonophysics, v. 192, p. 41–56.

Teskey, D. J., 1993, The aeromagnetic survey program of the Geological Survey of Canada: contribution to regional geological mapping and mineral exploration: Canadian Journal of Earth Sciences, v. 30, p. 243–260.

Wheeler, J., Hoffman, P., Card, K., Davidson, A., Sanford, B., Okulitch, A., and Roest, W., 1996, Geological map of Canada / Carte géologique du Canada:, accessed at Geological Survey of Canada, “A” Series Map 1860A, 1996, 3 sheets; 1 CD-ROM.

Wickham, H., 2014, Tidy data: Journal of Statistical Software, v. 59, p. 1–23.

Wickham, H., Averick, M., Bryan, J., Chang, W., McGowan, L., Francois, R., Grolemund, G., Hayes, A., Henry, L., Hester, J., Kuhn, M., Pedersen, T., Miller, E., Bache, S., et al., 2019, Welcome to the tidyverse: The Journal of Open Source Software, v. 4, p. 1686.

Yuan, H., French, S., Cupillard, P., and Romanowicz, B., 2014, Lithospheric expression of geological units in central and eastern North America from full waveform tomography: Earth and Planetary Science Letters, v. 402, p. 176–186.